J. Phys. B: At. Mol. Phys. 17 (1984) 3677–3691. Printed in Great Britain

The relative intensities of hydrogen-like fine structure

G J Tallents

Laser Physics Laboratory, Department of Engineering Physics, Research School of Physical Sciences, Australian National University, Canberra, ACT 2601, Australia

Received 5 March 1984

Abstract. The ratio of the intensities of the Lyman alpha ($n = 2 \rightarrow 1$), Balmer alpha ($n = 3 \rightarrow 2$) and Balmer beta ($n = 4 \rightarrow 2$) fine structure components of hydrogen-like ions emitted from plasmas of various atomic number Z is examined. It is shown that the fine structure intensities of Lyman alpha can only be deduced assuming statistical equilibrium between the fine structure sub-levels of quantum state $n = 2$ for electron densities $N_e \gtrsim 10^{13} Z^9$ cm^{-3}, while the fine structure intensities of Balmer alpha and beta can only be deduced assuming statistical equilibrium between the sub-levels of $n = 3$ and 4 respectively for $N_e \gtrsim 10^{12} Z^9$ cm^{-3}. At low electron densities ($N_e \lesssim 10^3 Z^9$ cm^{-3} for Lyman alpha, $N_e \lesssim 10^7 Z^9$ cm^{-3} for Balmer alpha and beta), the fine structure intensities are given by a coronal-like model, where collisional processes into the sub-levels are balanced by radiative de-excitation. At intermediate electron densities, the Lyman alpha, Balmer alpha and Balmer beta fine structure ratios can vary rapidly with N_e and should be useful as electron density diagnostics.

1. Introduction

Measurements of the relative intensities of closely spaced spectral lines can be very effective in diagnosing plasma conditions. The relative intensities of such lines are convenient to measure as only a limited wavelength range needs to be observed and intensity calibration at different wavelengths of the recording spectrograph is not required. Measurements of the relative intensities of resonance, intercombination and dielectronic satellite lines in the spectra of helium-like ions (e.g. Boiko *et al* 1979, Kallne *et al* 1983, Lunney 1983) and of the relative intensities of dielectronic satellite lines in the spectra of hydrogen-like ions (e.g. Boiko *et al* 1979, Seely and Lunney 1982) have been widely used as plasma density diagnostics. The relative intensities of the hydrogen-like Lyman alpha doublet components have also been employed as a plasma density diagnostic (Vinogradov *et al* 1974, 1977, Boiko *et al* 1978, 1979, Skobelev *et al* 1978).

In this paper, the relative intensities of the fine structure components of hydrogen-like Lyman alpha, Balmer alpha and Balmer beta lines are evaluated as functions of plasma density (and to a lesser extent plasma temperature) for atomic number Z plasmas in the range $Z = 2$ to 15. This paper presents the first comprehensive calculations of the Lyman alpha and Balmer alpha doublet intensity ratios for a range of atomic numbers and the first calculations for Balmer beta. Values of the Lyman alpha doublet ratio for $Z = 12$–15 (Vinogradov *et al* 1977, Boiko *et al* 1978, 1979) and the Balmer alpha doublet ratio for $Z = 2$, 6 and 14 (Tallents 1984) have been calculated before, but are included here for completeness. The hydrogen-like fine structure ratios should prove useful as density diagnostics in a wide range of plasma experiments, but this paper is aimed primarily at laser-produced plasmas which generally consist of one element and which are usually recombining.

2. Method

To evaluate the intensities of fine structure lines, it is necessary to calculate the population densities of the upper quantum sub-levels. The population density of the principle quantum number $n = n_p$ fine structure sub-levels of the hydrogen-like ion can be obtained by considering the processes populating and depopulating each sub-level. Denoting the populations of the $n = n_p$ fine structure sub-levels by N_i, we can write

$$-N_i\left[N_e\left(\sum_{j\neq i} C_{ij}\right)+A_i\right]+N_e\sum_{k\neq i} N_k C_{ki} = -Q_i \quad (1)$$

where C_{ij} is the rate coefficient for collision induced transitions between sub-levels i and j, A_i is the transition probability for radiative decay and collisional transitions to quantum states $n \neq n_p$ of sub-level i and Q_i is the rate of population of sub-level i from quantum states $n \neq n_p$ due to collisional and radiative processes. Radiative transitions between the sub-levels can be neglected as the transition probabilities are very small due to the small energy differences between sub-levels (Wiess *et al* 1966).

In order to solve equation (1) for population densities N_i, values for A_i, Q_i and C_{ij} need to be determined for the hydrogen-like ions. The values of A_i and Q_i have been calculated using a collisional–radiative code (Tallents 1976) developed to calculate the population densities of quantum states following the model of McWhirter and Hearn (1963). For conditions where the value of A_i is important in the present calculations, collisional excitation or de-excitation from a sub-level to a quantum state $n \neq n_p$ is small compared with radiative decay to the $n < n_p$ quantum states. The values of A_i are dominated by radiative transition probabilities as given by Wiess *et al* (1966). The rate Q_i of population of sub-levels from quantum states $n \neq n_p$ is taken to be proportional to the statistical weight ω_i of the final states. This can be shown to be reasonably accurate for a recombining plasma where collisional and radiative population of quantum state $n = n_p$ from states $n \neq 1$ dominates (Vinogradov *et al* 1977 and see § 4.4). Vainshtein (1975) has shown that collisional excitation rate coefficients are often proportional to the statistical weight of the final quantum state when the energy interval is close to the plasma electron temperature and exchange is taken into account. By taking $Q_i \propto \omega_i$, the fine structure sub-levels of each quantum state n_p can be considered individually (for each spectral line studied) and it is not necessary to simultaneously treat the fine structure sub-levels of a large number of quantum states. Similarly, the absolute values of Q_i are not important as only the relative values of Q_i (taken to be proportional to ω_i) affect the fine structure ratios.

Each rate coefficient C_{ij} has a contribution from an electron collision induced (C^e_{ij}) and ion collision induced (C^i_{ij}) rate coefficient such that

$$C_{ij} = C^e_{ij} + (1/Z_{eff})C^i_{ij} \quad (2)$$

where Z_{eff} is the degree of plasma ionisation which is taken to be the ratio of the electron density to the ion density. The energies between the fine structure sub-levels are always very much smaller than the temperatures of ions or electrons in the plasma under consideration, so using the principle of detailed balance

$$C_{ij}^{e,i} = (\omega_j/\omega_i)C_{ji}^{e,i} \tag{3}$$

where ω_i is the statistical weight of the sub-level i.

For the results of this paper, the rate coefficients C_{ij}^{e} and C_{ij}^{i} are calculated following Shevelko *et al* (1976, 1977). These authors evaluated expressions for the C_{ij}^{e} and C_{ij}^{i} values using the Born approximation for dipole allowed collision induced transitions with a model potential $V(R)$ for the hydrogen-like ions of the form in atomic units $V(R) = \lambda R/(R^2+R_0)^{3/2}$ for the C_{ij}^{e} evaluation and $V(R) = \lambda/R^2$ for the C_{ij}^{i} evaluation. The rate coefficients between optically allowed sub-levels are much greater than the rate coefficients between optically forbidden transitions and hence the C_{ij} values for optically forbidden transitions can be approximated to zero. Converting the results of Shevelko *et al* (1977) to CGS units, we have

$$C_{ij}^{e} = 2.7\times10^{-2}\lambda^2 f(\alpha)(R_0\Delta E_{ij})^{-1} \tag{4}$$

$$C_{ij}^{i} = 10^{-4}\lambda^2\psi(y)(M/T_i)^{1/2} \tag{5}$$

where ΔE_{ij} is the energy difference between the fine structure sub-levels in cm^{-1} (see e.g. Bashkin and Stoner 1975), T_i is the ion temperature in K and M is the atomic weight of the plasma ions. For the quantum state transitions n, $l \to n$, $(l+1)$ in hydrogen-like ions

$$\lambda^2 = 3(l+1)n^2[n^2-(l+1)^2][4(2l+1)Z^2]^{-1} \tag{6}$$

$$R_0 = n^2/Z. \tag{7}$$

To evaluate C_{ij}^{e}, we use

$$\alpha = 391\,T_e^{1/2}/(R_0\Delta E_{ij}) \tag{8}$$

where T_e is the electron temperature in K. The asymptotic $\alpha\to\infty$ expression of Shevelko *et al* (1977) is used for $f(\alpha)$, that is

$$f(\alpha) = (\ln\alpha - 0.321)/\alpha. \tag{9}$$

For the results of this paper, $\alpha > 5$ and equation (9) gives $f(\alpha)$ to within 10% of more complete numerical evaluations also given by Shevelko *et al* (1977).

For the evaluation of C_{ij}^{i}

$$y = 2.45\times10^4 ZZ_{eff}\Delta E_{ij}M^{1/2}/T_i^{3/2}. \tag{10}$$

Again the asymptotic $y\to\infty$ expression of Shevelko *et al* (1977) is used for $\psi(y)$

$$\psi(y) = 73y^{0.2}\exp(-2.7y^{0.4}). \tag{11}$$

Interestingly, for $y \leqslant 0.1$ where equation (11) would, at first, be thought to give a poor approximation for $\psi(y)$, the values for $\psi(y)$ obtained using equation (11) are only at most an order of magnitude smaller than values from an expression for $\psi(y)$ obtained by Shevelko *et al* (1977) assuming $y\to 0$. In fact, more complete numerical calculations by Shevelko *et al* (1977) predict values of $\psi(y)$ for small y which are closer to the values given by equation (11) (usually to within a factor two) than to the $\psi(y)$, $y\to 0$ approximation.

For low atomic number ($Z = 2$–6), the rate coefficients C_{ij} are dominated by ion collision induced transitions, but for higher Z ($Z > 6$) with larger energy gaps between the fine structure sub-levels, electron collision induced transitions become dominant.

The results presented in this paper for lower Z ($Z = 2$–6) are, therefore, likely to be less accurate than the higher Z ($Z > 6$) results because of the greater possible inaccuracies (discussed above) in the ion collision induced rate coefficients C^{i}_{ij} compared with the electron collision induced rate coefficients C^{e}_{ij}. The degree of plasma ionisation Z_{eff} (assumed equal to Z for this paper) only affects the present results for low atomic number ($Z = 2$–6) plasmas where ion collision induced transitions between the sub-levels dominate. For low Z, the results depend mainly on the ion density ($= N_e / Z_{eff}$) rather than the electron density N_e.

3. Results

3.1. Lyman alpha

The Lyman alpha transition 1s–2p of the hydrogen-like ion has two fine structure components corresponding to the transitions $1s_{1/2}$–$2p_{1/2}$ and $1s_{1/2}$–$2p_{3/2}$ (see figure 1). The relative intensities β_1 of the Lyman alpha fine structure components are given by

$$\beta_1 = \frac{I(1s_{1/2} - 2p_{1/2})}{I(1s_{1/2} - 2p_{3/2})} = \frac{N_{2p_{1/2}}}{N_{2p_{3/2}}}. \tag{12}$$

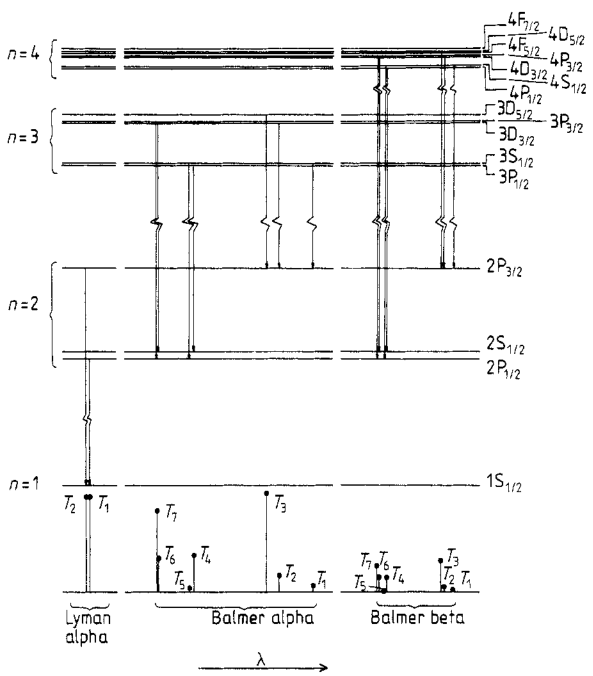

Figure 1. Grotrian diagram showing the fine structure of Lyman alpha, Balmer alpha and Balmer beta and associated quantum sub-levels. The radiative transition probabilities T_m ($m = 1$, 2 for Lyman alpha, $m = 1, 2, \ldots, 7$ for Balmer alpha and beta) and relative wavelengths for each fine structure component are indicated underneath the Grotrian diagram. The transition probabilities for Lyman alpha (T_1 and T_2) are reduced by a factor of ten compared with the scale used for those of Balmer alpha and beta.

Denoting the quantum states $2p_{1/2}$, $2s_{1/2}$ and $2p_{3/2}$ (in increasing energy) by $i=1$, 2 and 3, using equation (3) and approximating the rate coefficients for the optically forbidden transition $2p_{1/2} \leftrightarrows 2p_{3/2}$ by $C_{13}=C_{31}=0$, equations (1) ($i=1$, 2 and 3) can be simultaneously solved to give analytic expressions for the fine structure sub-level population densities N_1, N_2 and N_3. The fine structure ratio β_1 is given by

$$\beta_1 = N_1/N_3 = \tfrac{1}{2}\left(1 + \frac{(2/C_{23} - 1/C_{12})(1 - A_2/A_1)}{(1 + A_2/A_1)2/C_{23} + 3/C_{12} + 4N_e/A_1 + 2A_2/(N_e C_{23} C_{12})}\right) \tag{13}$$

upon setting $A_3 = A_1$. The validity of equation (13) has been checked using a computer algebraic manipulation package (Hearn 1973) and also by numerical solution of equation (1).

The value of A_2 is dominated by the transition probability for two-photon decay of the $i=2$ ($2s_{1/2}$) sub-level. Two-photon decay of the $2s_{1/2}$ sub-level was first considered by Breit and Teller (1940) and has been calculated by many authors to have a transition probability of $8.23Z^6\ \mathrm{s}^{-1}$ in the non-relativistic approximation, a value changed by less than 1% by relativistic corrections for $Z \leqslant 15$ (Marrus and Mohr 1978, Gould and Marrus 1983). The $2s_{1/2}$ sub-level also decays by a single photon relativistic-magnetic decay which scales approximately as Z^{10}, but which should not affect the value of A_2 by more than 1% for $Z \leqslant 15$. The value of A_1 ($=A_3$) is dominated by the allowed electric dipole transition 1s–2p which has a transition probability $6.27 \times 10^8 Z^4\ \mathrm{s}^{-1}$ (Wiess *et al* 1966).

Using equation (13), the above values for A_1 and A_2, and the expression for the rate coefficients C_{23} and C_{12} given in § 2, values of β_1 have been calculated for atomic number Z plasmas in the range $Z=2$–15 as a function of electron density N_e (figure 2). We assume that the electron and ion temperatures are equal and that $Z_{\mathrm{eff}} = Z$. The β_1 values for $Z=12$–15 are in good agreement with calculations by Boiko *et al* (1978, 1979).

At 'high' electron densities ($N_e \gg \tfrac{1}{4}A_1(2/C_{23} + 3/C_{12})$), collisional transitions between sub-levels are sufficient to cause the sub-level populations to be in statistical equilibrium. The value of $\beta_1 = N_1/N_3 = \omega_1/\omega_3 = 0.5$ (as shown in figure 2). At 'low' electron densities ($N_e \ll 2A_2/(2C_{12} + 3C_{23})$), the sub-level populations are given by a coronal-like balance between collisional processes (Q_i) from quantum states $n \neq 2$ populating the sub-level i and radiative decay ($N_i A_i$), that is

$$N_i = Q_i/A_i = \omega_i Q_1/\omega_1 A_1 \tag{14}$$

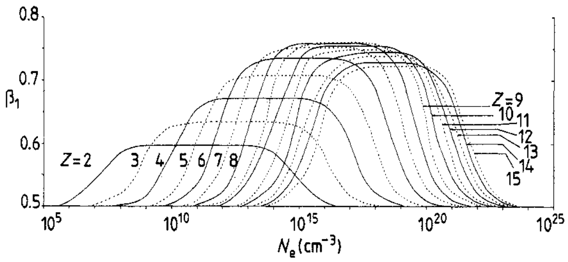

Figure 2. The ratio β_1 of the intensity of the doublet components of the hydrogen-like Lyman alpha line as a function of electron density N_e for various atomic number Z (as indicated). The electron and ion temperatures are assumed equal to a value of 0.2 of the ionisation potential of each ion, that is $3.157 \times 10^4 Z^2$ K.

for $i = 1$ or 3. Again the value of $\beta = N_1/N_3 = \omega_1/\omega_3 = 0.5$ (as also shown in figure 2). At 'intermediate' electron densities

$$(2A_2/(2C_{12}+3C_{23}) \ll N_e \ll \tfrac{1}{4}A_1(2/C_{23}+3/C_{12}))$$

from equation (13)

$$\beta_1 = \beta_{max} = \tfrac{1}{2}[1+(2C_{12}-C_{23})/(2C_{12}+3C_{23})] \tag{15}$$

as $A_2 \ll A_1$. The value of β_{max} depends on the values of C_{23} and C_{12} and hence on the ion and electron temperatures of the plasma (figure 3). The β_1 value is useful as a diagnostic of density in the two electron density regimes where β_1 varies rapidly with N_e from β_{max} to 0.5 (see figure 2).

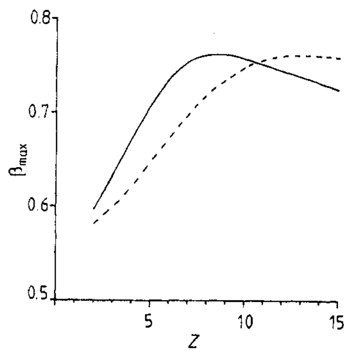

Figure 3. The maximum value (β_{max}) of the ratio β_1 of the intensity of the doublet components of Lyman alpha as a function of atomic number Z. The electron and ion temperatures are assumed equal to a value of 0.2 of the ionisation potential of each ion, that is $3.157 \times 10^4 Z^2$ K (full curve) or 0.5 of the ionisation potential of each ion, that is $7.891 \times 10^4 Z^2$ K (broken curve).

From the results of figure 2, it has been found empirically that the $n = 2$ sub-level populations are proportional to their statistical weights for electron densities $N_e \gtrsim 10^{13} Z^9$ cm^{-3}. Similarly the coronal-like model is valid for electron densities $N_e \lesssim 10^3 Z^9$ cm^{-3}. These densities are largely independent of the plasma temperature. The major effect of varying plasma temperature is to change the value of β_{max}. β_{max} varies by up to 10% over the temperature range 0.2 to 0.5 of the ionisation potential (see figure 3). From figure 2 it can be seen that a temperature uncertainty of this magnitude could lead to errors in deduced densities of up to an order of magnitude.

3.2. Balmer alpha

The Balmer alpha transition $n = 3 \rightarrow 2$ of the hydrogen-like ion consists of seven fine structure components grouped to give the appearance of a doublet (see figure 1). The intensity of the fine structure components depends on the population density N_i of the $n = 3$ upper quantum sub-level associated with the transition and on the transition probability T_m (see Kuhn 1969, Wiess *et al* 1966) for the particular fine structure component (figure 1). The ratio β_2 of the doublet componets of Balmer alpha is given by

$$\beta_2 = \frac{N_2 T_1 + N_3 T_2 + N_5 T_3}{N_1 T_4 + N_2 T_5 + N_4 T_6 + N_3 T_7} \tag{16}$$

where the population densities N_i of the quantum state apply to the sub-levels designated by $i = 1, 2, \ldots, 5$ (i increasing with increasing energy of the sub-level).

The coupled linear equations (1) ($i = 1, 2, \ldots, 5$) have been solved numerically for N_i for the quantum state $n = 3$ using values for A_i, Q_i and C_{ij} as outlined in § 2 and assuming the electron and ion temperatures are equal and that $Z_{eff} = Z$. Calculated values of β_2 as a function of electron density N_e are plotted in figure 4. At 'high' electron densities the sub-level population densities N_i are proportional to the statistical weight ω_i of the sub-levels and hence from equation (16), $\beta_2 = 1.240$. At 'low' electron densities, the sub-level populations N_i are given by a coronal-like balance between the rate Q_i of population of the sub-levels from quantum states $n \neq 3$ and the rate of radiative de-excitation ($N_i A_i$), that is

$$N_i = Q_i / A_i.$$

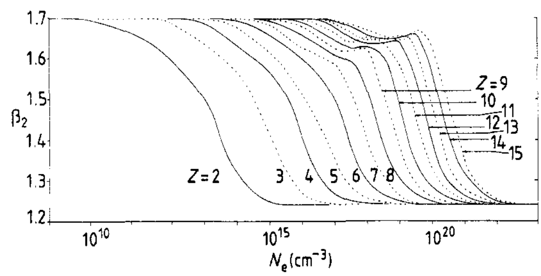

Figure 4. The ratio β_2 of the intensity of the doublet components of the hydrogen-like Balmer alpha line as a function of electron density N_e for various atomic number Z (as indicated). The electron and ion temperatures are assumed equal at a value of 0.2 of the ionisation potential of each ion, that is $3.157 \times 10^4 Z^2$ K.

Taking Q_i to be proportional to the statistical weight ω_i and using equations (16) gives $\beta_2 = 1.698$, in agreement with the calculations shown in figure 4.

From the results of figure 4, it has been found empirically that the $n = 3$ sub-level populations are proportional to their statistical weights for electron densities $N_e \geqslant 10^{12} Z^9$ cm^{-3}. Similarly, the coronal-like model is valid for electron densities $N_e \leqslant 10^7 Z^9$ cm^{-3}. At intermediate electron densities

$$(10^7 Z^9 \text{ cm}^{-3} \leqslant N_e \leqslant 10^{12} Z^9 \text{ cm}^{-3}),$$

the value of β_2 changes rapidly with electron density and could be used as a diagnostic of electron density. The β_2 values for a given N_e and Z vary little with plasma temperature, particularly for higher Z plasmas (figure 5).

3.3. Balmer beta

The Balmer beta transition $n = 4 \rightarrow 2$ of the hydrogen-like ion consists of seven fine structure components grouped to give the appearance of a doublet in a similar manner

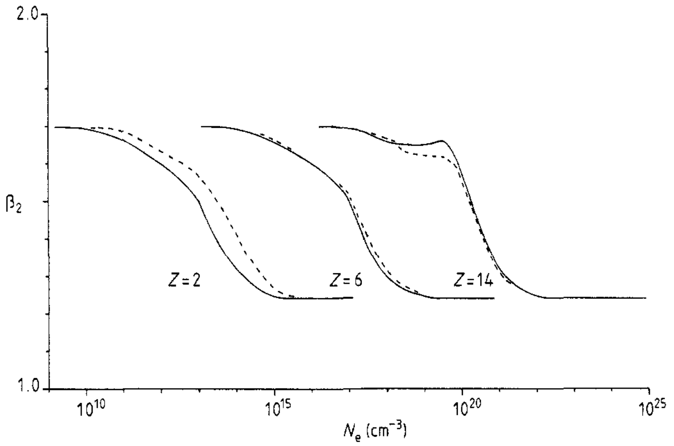

Figure 5. Values of β_2 showing the effect of varying plasma temperatures. The electron and ion temperatures are assumed equal at a value of 0.2 of the ionisation potential of each ion, that is $3.157 \times 10^4 Z^2$ K (full curves) or 0.5 of the ionisation potential of each ion, that is $7.891 \times 10^4 Z^2$ K (broken curves).

to the Balmer alpha line (see figure 1). The ratio β_3 of the doublet components of Balmer beta is given by

$$\beta_3 = \frac{N_2 T_1 + N_3 T_2 + N_6 T_3}{N_1 T_4 + N_2 T_5 + N_4 T_6 + N_3 T_7} \tag{17}$$

where the population densities N_i of the quantum sub-levels of the $n = 4$ quantum state apply to the sub-levels designated by $i = 1, 2, \ldots, 7$ (i increasing with increasing energy of the sub-level). The coupled linear equations (1) ($i = 1, 2, \ldots, 7$) have been solved numerically for N_i for the quantum state $n = 4$ using values for A_i, Q_i and C_{ij} as outlined in § 2. The electron and ion temperatures are taken to be equal and it is assumed that $Z_{\mathrm{eff}} = Z$.

Calculated values of β_3 as a function of electron density N_e are plotted in figure 6. At 'high' electron densities the sub-level population densities N_i are proportional

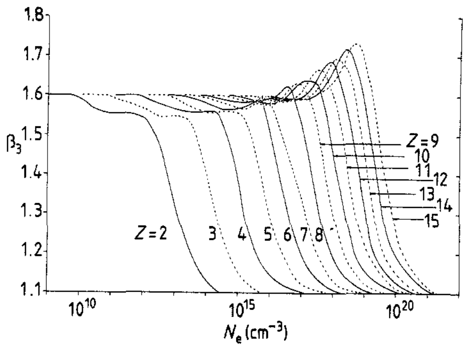

Figure 6. The ratio β_3 of the intensity of the doublet components of the hydrogen-like Balmer beta line as a function of electron density N_e for various atomic numbers Z (as indicated). The electron and ion temperatures are assumed equal at a value of 0.2 of the ionisation potential of each ion, that is $3.157 \times 10^4 Z^2$ K.

to the statistical weight ω_i at the sub-levels and hence from equation (17), $\beta_3 = 1.107$. At 'low' electron densities, the sub-level populations are given by a coronal-like balance and $\beta_3 = 1.601$. The electron density regimes where the statistical equilibrium or coronal models are valid scale in the same way as for the Balmer alpha line (i.e. $N_e \gtrsim 10^{12}Z^9\ \text{cm}^{-3}$ or $N_e \lesssim 10^7 Z^9\ \text{cm}^{-3}$ respectively). At the intermediate electron densities ($10^7 Z^9\ \text{cm}^{-3} \lesssim N_e \lesssim 10^{12}Z^9\ \text{cm}^{-3}$), the value of β_3 changes rapidly with electron density and at least in the upper density range (N_e near $10^{12}Z^9\ \text{cm}^{-3}$) could be used as a diagnostic of electron density. The β_3 values (like β_2) for a given N_e and Z vary little with plasma temperature (figure 7).

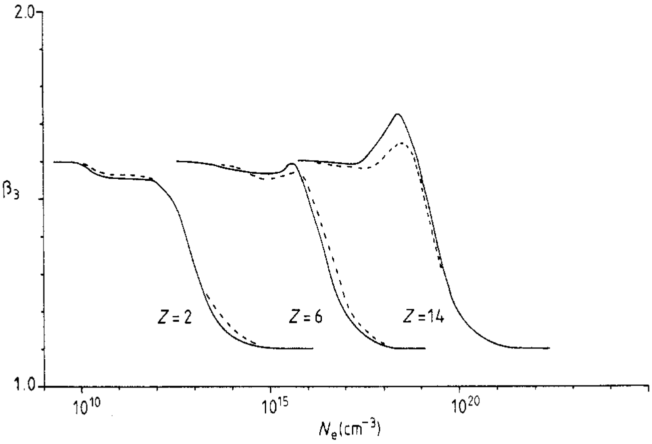

Figure 7. Values of β_3 showing the effect of varying plasma temperatures. The electron and ion temperatures are assumed equal at a value of 0.2 of the ionisation potential of each ion, that is $3.157 \times 10^4 Z^2$ K (full curves) or 0.5 of the ionisation potential of each ion, that is $7.891 \times 10^4 Z^2$ K (broken curves).

4. Discussion

4.1. β_1, β_2 and β_3 as density diagnostics

Employment of the hydrogen-like fine structure ratios β_1, β_2 and β_3 as plasma density diagnostics should prove useful in a wide range of plasma experiments. However, the Balmer alpha and beta fine structure ratios (β_2 and β_3) appear to have significant advantages for laser-produced plasmas as density diagnostics over the previously employed (e.g. Boiko *et al* 1978, 1979) Lyman alpha ratio (β_1). The Balmer alpha and beta fine structure doublets can be more easily resolved than the Lyman alpha doublet (see the discussion below) and Balmer alpha and beta are much more likely to be optically thin than is Lyman alpha (the effect of opacity is discussed at the end of this section). The ratios β_2 and β_3 are also less dependent on plasma temperature than is β_1 (compare figures 5 and 7 with figure 3).

To use the hydrogen-like fine structure ratios as density diagnostics it is, of course, necessary to spectrally resolve the Lyman alpha, Balmer alpha or Balmer beta doublets (wavelength separations 5 mÅ, 130 mÅ and 80 mÅ respectively). In general, this becomes easier with increasing atomic number Z as the Lyman alpha, Balmer alpha and Balmer beta wavelengths (λ_1, λ_2, λ_3 respectively) decrease ($\lambda_1 \simeq 1215/Z^2$ Å,

$\lambda_2 \simeq 6560/Z^2$ Å, $\lambda_3 \simeq 4860/Z^2$ Å), while the doublet separations remain approximately constant. The Balmer alpha and beta doublets can be expected to be resolvable if thermal Doppler broadening dominates and ion temperatures are less than about $0.1Z^5$ eV (e.g. 3 eV for $Z=2$). However, the Lyman alpha doublet will only be resolvable for ion temperatures less than about $0.003Z^5$ eV (e.g. 0.1 eV for $Z=2$). The Lyman alpha, Balmer alpha and Balmer beta doublets should all be resolvable if Stark broadening dominates for the electron density range considered in this paper ($N_e \leqslant 10^{13}Z^9$ cm^{-3}; see, for example, equation (4) of Irons 1973).

The curves for β_1, β_2 and β_3 (figures 2–7) shift linearly along the electron density axis with variations of the C_{ij} values. This means that the maximum error which could be introduced in an electron density measurement by inaccurate rate coefficients is equal to the maximum error in C_{ij}, that is approximately a factor of two in the present calculations. In practice, the error will usually be smaller than a factor of two because most of the rate coefficients in a given calculation are accurate to approximately 10% (see § 2; the Born approximation is quite accurate for temperatures much greater than the energy gap). In general, the results presented for lower Z ($Z=2$–6) are less accurate than for higher Z ($Z>6$) because of the greater possible inaccuracies in the ion collision induced rate coefficients (which dominate at low Z) compared with the electron collision induced rate coefficients (which dominate at high Z).

Self-absorption can readily change the measured β_1, β_2 or β_3 ratios in an experiment. Irons (1980a, b) has pointed out the problems of interpreting fine structure ratios when the lines are not optically thin. Assuming a uniform plasma along the line of sight, the intensity ratio I_r/I_b of the high (red) to low (blue) wavelength components of a doublet emitted from a plasma can be obtained by solving the equation of radiative transfer (Tallents 1982). We have

$$\frac{I_r}{I_b} = 1 + \frac{1-\exp[\tau(1-\beta)]}{\exp\tau - 1} \tag{18}$$

where τ is the optical depth of the lower wavelength component and β is one of the ratios β_1, β_2 or β_3. Setting $\beta = 1.7$, it can be shown from equation (18) that $\tau < 0.05$ is required for I_r/I_b to vary by less than 2% from β. Large amounts of self-absorption can completely alter the value of I_r/I_b from the optically thin value (β). For example, for $\beta = 1.7$, $\tau = 1$ we have $I_r/I_b = 1.29$. Clearly, it is essential that the plasma is close to optically thin for the spectral line being investigated if the doublet ratio is to be an accurate density diagnostic. Balmer alpha and beta are much more likely to be optically thin than Lyman alpha because of the greater transition probability of Lyman alpha and, in most plasmas, greater density of the hydrogen-like ground state compared with the first excited quantum state.

4.2. Population density calculations

The collisional–radiative codes developed to calculate the population densities of excited quantum states of hydrogen-like ions have been written (with one exception known to the author—the code by Hutcheon and McWhirter 1973) assuming that the fine structure sub-levels are populated according to their statistical weights. It has been shown in this paper that this assumption is only valid for electron densities $N_e \geqslant 10^{13}Z^9$ cm^{-3} (for $n=2$) and $N_e \geqslant 10^{12}Z^9$ cm^{-3} (for $n=3$ and 4). At lower electron densities, the populations of the sub-levels with less probability of radiative decay have been found to be much greater than the value an assumption of statistical equilibrium between sub-levels would predict. This is particularly apparent with the $2s_{1/2}$ sub-level which can mainly decay radiatively by only a two-photon process (Marrus and Mohr 1978). Using the coronal model and assuming the sub-levels are populated according to their statistical weight, the $n=2$ quantum state will have a total population $N_{tot}=Q_{tot}/A(2,1)$ where Q_{tot} is the total collisional excitation rate into the $n=2$ quantum state and $A(2,1)$ is the total radiative transition probability for the $n=2\rightarrow 1$ transition assuming the sub-levels are populated according to their statistical weight (as given by e.g. Wiess *et al* 1966). However, assuming the individual quantum sub-level populations are given by a coronal-like model, the total population of the $n=2$ quantum state will be

$$N_{sum}=\sum_i Q_i/A_i \qquad (19)$$

where the summation is over the quantum state sub-levels. For $n=2$, the ratio $N_{sum}/N_{tot}=1.43\times 10^7/Z^2$. This means that the population of the $n=2$ quantum state of a hydrogen-like ion of atomic number Z can exceed by up to a factor $1.43\times 10^7/Z^2$ the population predicted by a coronal model or collisional–radiative code (e.g. Tallents 1976) which assumes statistical equilibrium between the sub-levels. For $n>2$, the equivalent ratios N_{sum}/N_{tot} are much smaller (2.77 for $n=3$ and 1.8 for $n=4$), but still possibly significant in some calculations.

The large enhancement of the population density of the 2s quantum sub-level in the coronal-like regime ($N_e\leqslant 10^3Z^9\,\mathrm{cm}^{-3}$) suggests that the flux I_{2s} of two-photon emission by the decay of the 2s sub-level could approach the flux I_{2p} by Lyman alpha emission from the 2p sub-levels. The ratio of the number of photons emitted by two-photon and Lyman alpha emission will be

$$\frac{I_{2s}}{I_{2p}}=2\frac{N_2}{N_1+N_3}\frac{A_2}{A_1} \qquad (20)$$

where the factor two allows for the emission of two photons (rather than one) in two-photon decay. When the population of the sub-levels N_1, N_2 and N_3 are given by the coronal-like model (i.e. $N_i=Q_i/A_i$), we have $I_{2s}/I_{2p}=2\omega_2/(\omega_1+\omega_3)=\frac{2}{3}$. Such a high flux of two-photon emission compared with Lyman alpha emission could be important in low density plasmas of astrophysical interest such as gaseous nebulae (Breit and Teller 1940, Gerola and Panagia 1968). In gaseous nebulae, the Lyman alpha emission is likely to be optically thick (with large opacity), but to a first approximation I_{2s}/I_{2p} should still be approximately $\frac{2}{3}$. While the enhanced 2p population caused by photo-excitation (1s–2p) will result in extra photon emission, the self-absorption producing the photo-excitation will reduce the number of photons escaping from the plasma. Using the escape factor (net radiative bracket) approach (see e.g. Irons 1980b), the population densities N_1, N_3 become

$$N_1=Q_1/(\Lambda_e A_1)$$
$$N_3=Q_3/(\Lambda_e A_1) \qquad (21)$$

where Λ_e is the net radiative bracket for the Lyman alpha emission from the plasma. Equation (19) then becomes

$$\frac{I_{2s}}{I_{2p}}=2\frac{\omega_2/A_2}{(\omega_1+\omega_3)/(\Lambda_e A_1)}\frac{A_2}{\Lambda_f A_1}=\frac{2}{3} \qquad (22)$$

upon equating the escape probability Λ_f (for the line of sight) to the net radiative bracket Λ_e (see Irons 1978).

From the above discussion, it could perhaps be thought that Lyman alpha, Balmer alpha and Balmer beta radiation flux calculations which assume statistical equilibrium between sub-levels may be in serious error for low density plasmas. In fact, the low probability of photon emission from sub-levels with populations enhanced above the statistical equilibrium values means that errors in calculated spectral line intensities will be only of the order of the differences in β_1, β_2 and β_3 from values assuming statistical equilibrium between the fine structure sub-levels. Errors of less than or about 50% can thus be expected for calculations of Lyman alpha, Balmer alpha and Balmer beta emission in low density plasmas if the quantum sub-levels are assumed to be in statistical equilibrium.

Sampson (1977) examined the plasma conditions where statistical equilibrium between sub-levels of hydrogen-like principal quantum numbers would be valid by comparing collisional rates between sub-levels with radiative decay rates to lower quantum states. His results agree reasonably well with the present calculations for $n=2$ and 3, though predicting a scaling $N_e \propto Z^8$ (rather than $N_e \propto Z^9$ as we have found empirically). However, our results for $n=4$ require at least an order of magnitude greater electron density to achieve statistical equilibrium than predicted by Sampson (1977). This difference may be due to the different collisional rate coefficients between sub-levels used here and by Sampson (1977).

4.3. *Implications*

One implication of the β_1, β_2 and β_3 ratios varying from the values to be expected if the fine structure sub-levels are in statistical equilibrium is that the usual wavelengths quoted for the weighted line centres (e.g. Bashkin and Stoner 1975) are inappropriate. For Lyman alpha with $\beta_1 = 0.7$, the weighted line centre will shift +0.4 mÅ compared with the statistical equilibrium wavelength with $\beta_1 = 0.5$. The weighted line centre of Balmer alpha for $\beta_2 = 1.7$ will shift +10 mÅ compared with the statistical equilibrium wavelength (with $\beta_2 = 1.24$) and the weighted line centre of Balmer beta for $\beta_3 = 1.6$ will shift +6 mÅ compared with the statistical equilibrium wavelength (with $\beta_3 = 1.1$). These shifts in the weighted line centres are independent of atomic number Z and hence are likely to be important in high-Z plasmas if, for example, the unresolved doublets are used as wavelength standards.

The ratio of the intensity of the doublet components of Balmer alpha have been used to deduce optical gain for the C VI Balmer alpha line at 182 Å in a laser-produced plasma (Jacoby *et al* 1981). In the presence of gain both of the doublet components are amplified with a gain coefficient proportional to the emissivity of the particular doublet component. If G is the gain of the low wavelength Balmer alpha doublet component and we assume a uniform gain along the plasma length L, the intensity ratio I_r/I_b of the high (red) to low (blue) wavelength components of the Balmer alpha doublet is given by

$$\frac{I_r}{I_b} = 1 + \frac{\exp[GL(\beta_2 - 1)] - 1}{1 - \exp(-GL)} \tag{23}$$

upon replacing τ with $-GL$ in equation (18). The ratio I_r/I_b is a strong function of the gain coefficient G, but clearly is also extremely sensitive to the value of β_2. Computer modelling (Jacoby *et al* 1982) shows that most of the C VI Balmer alpha gain reported by Jacoby *et al* (1981) is produced at electron densities $N_e \simeq 1\text{–}2 \times 10^{19}$ cm^{-3}. Figures 4 and 5 show that for $N_e \gtrsim 10^{19}$ cm^{-3}, $\beta_2 = 1.24$ (the statistical value). It seems, therefore, that the C VI Balmer alpha gains deduced by Jacoby *et al* (1981) from the intensity ratios of the doublet components assuming $\beta_2 = 1.24$ should not be affected by departures of the sub-level populations from statistical equilibrium.

4.4. *Validity of the β_1, β_2 and β_3 calculations*

It has been assumed for this paper that the rate of population Q_i of the sub-levels from other principal quantum number states is proportional to the statistical weight ω_i of the final quantum sub-level. This can be shown to be often correct when electron temperatures are close to the energy gaps between principal quantum number states and collisional population of the sub-levels dominates (Vainshtein 1975). Moreover, it can also be shown that Q_i is approximately proportional to ω_i when radiative populating mechanisms are important. Using the coronal-like model where the sub-level populations $N_i = Q_i/A_i$ (see § 3) and assuming the dominant mechanism populating the $n = 2$, 3 or 4 quantum sub-levels is radiative recombination from quantum sub-levels of $n = 3$, 4 or 5 respectively (and for a first approximation that the $n = 5$ quantum sub-levels are populated according to their statistical weight), we have $\beta_1 = 0.503$, $\beta_2 = 1.90$ and $\beta_3 = 1.68$. These values are not significantly different to the values obtained for the coronal-like regime when collisional processes dominate ($\beta_1 = 0.5$, $\beta_2 = 1.70$ and $\beta_3 = 1.60$). When radiative processes are important, approximately similar variations of β_2 and β_3 can thus be expected to those shown in figures 4–7. Some results for the Lyman alpha doublet ratio when radiative recombination dominates have been presented by Vinogradov *et al* (1977). Similar variations of β_1 to those shown in figure 2 occur, except that the values of β_{max} can be greater.

There are not many published experimentally measured values of β_1, β_2 and β_3. Boiko *et al* (1978, 1979) have obtained good agreement of β_1 values measured from Lyman alpha emission of impurities in laser-produced plasmas with the values to be expected for the plasma conditions. However, though generally as expected, anomalous variations of β_1 have been reported by Kallne and Kallne (1982) and Kallne *et al* (1982) in Lyman alpha emission of high Z impurities from a tokamak plasma. The Balmer lines for $Z = 5\text{–}9$ emitted from a laser-produced plasma have been recorded by Nicolosi *et al* (1979). In their work, the doublet nature of the Balmer lines becomes better resolved with increasing Z as is to be expected. Also, close to the target their values of β_2 and β_3 increase with increasing distance from the target, as is consistent with decreasing electron density and the results of figures 4–7. However, at large distances from the target, values of β_2 and β_3 deduced from the published figures of Nicolosi *et al* (1979) appear to return to values $\beta_2, \beta_3 \simeq 1.0\text{–}1.2$, which are inconsistent with decreasing electron density with distance from the target and the calculations presented in this paper.

A possible explanation for the above experimental variations of β_1, β_2 and β_3 from expected values may be the failure in plasmas under certain conditions of the assumption that $Q_i \propto \omega_i$. It is possible that Q_i may not always be proportional to ω_i when Q_i is dominated by collisional excitation from the ground state (see e.g. Tully 1973). However, the presented β_1, β_2 and β_3 results should be accurate for recombining plasmas where the Q_i values can be expected to be dominated by collisional and radiative processes from excited quantum states.

5. Summary and conclusions

The ratio of the intensities of the hydrogen-like Lyman alpha, Balmer alpha and Balmer beta fine structure components emitted from plasmas of various atomic number Z have been examined. It has been shown that the fine structure intensities can only be deduced assuming statistical equilibrium between the fine-structure sub-levels for electron densities N_e greater than a certain minimum ($N_e \geqslant 10^{13} Z^9$ cm^{-3} for Lyman alpha and $N_e \geqslant 10^{12} Z^9$ cm^{-3} for Balmer alpha and beta). At lower electron densities, the fine structure ratios vary rapidly with N_e and should be useful as electron density diagnostics.

The Balmer alpha and beta fine structure ratios have some advantages as density diagnostics over the Lyman alpha ratio. The Balmer alpha and beta doublets can be more easily resolved than the Lyman alpha doublet and are more likely to be optically thin than is Lyman alpha. The Balmer alpha and beta fine structure intensities are also less dependent on plasma temperature than is Lyman alpha. Possible disadvantages in the use of the Balmer lines as density diagnostics compared with the use of Lyman alpha include the lower intensity of the Balmer emission and the possibly inconvenient wavelength of the Balmer alpha and beta lines. For $Z \leqslant 15$, the Balmer alpha and beta wavelengths are in the vacuum and extreme ultra-violet, necessitating the use of grazing-incidence spectrographs, while largely precluding the use of crystal spectrographs.

Implications of the fine structure ratios varying from the values obtained where the sub-levels are in statistical equilibrium have been discussed. It has been shown that the sub-level populations can be much greater than the assumption of statistical equilibrium predicts. In particular, the total $n=2$ quantum state population can be $1.43 \times 10^7/Z^2$ greater because of enhancement of the 2s population. It has also been shown that recent measurments of C VI Balmer alpha gain (Jacoby *et al* 1981, 1982) were probably not affected by departures of the sub-levels from statistical equilibrium.

References

Bashkin S and Stoner J O 1975 *Atomic Energy Levels and Grotrian Diagrams* vol 1 (Amsterdam: North-Holland)
Boiko V A, Pikuz S A and Faenov A Y 1979 *J. Phys. B: At. Mol. Phys.* **12** 1889–910
Boiko V A, Vinogradov A V, Pikuz S A, Skobelev I Y, Faenov A Y and Yukov E A 1978 *Sov. J. Plasma Phys.* **4** 54–8
Breit G and Teller E 1940 *Astrophys. J.* **91** 215–38
Gerola H and Panagia N 1968 *Astrophys. Space Sci.* **2** 285–301
Gould H and Marrus R 1983 *Phys. Rev.* A **28** 2001–25
Hearn A C 1973 *Reduce 2 User's Manual* (Utah: University of Utah Press)
Hutcheon R J and McWhirter R W P 1973 *J. Phys. B: At. Mol. Phys.* **6** 2668–83
Irons F E 1973 *J. Phys. B: At. Mol. Phys.* **6** 1562–81
—— 1978 *Mon. Not. R. Astron. Soc.* **182** 705–9
—— 1980a *Aust. J. Phys.* **33** 283–301
—— 1980b *J. Quant. Spectrosc. Radiat. Transfer* **24** 119–32
Jacoby D, Pert G J, Ramsden S A, Shorrock L D and Tallents G J 1981 *Opt. Commun.* **37** 193–6
Jacoby D, Pert G J, Shorrock L D and Tallents G J 1982 *J. Phys. B: At. Mol. Phys.* **15** 3557–80
Kallne E and Kallne J 1982 *AIP Conf. Proc. 94 X-ray and Atomic Inner-Shell Physics* 1982 ed B Craseman (New York: AIP) pp 463–78
Kallne E, Kallne J and Pradhan A K 1983 *Phys. Rev.* A **27** 1476–86
Kallne E, Kallne J and Rice J E 1982 *Phys. Rev. Lett.* **49** 330–3

Kuhn H G 1969 *Atomic Spectra* (London: Longman) pp 123 and 435
Lunney J G 1983 *J. Phys. B: At. Mol. Phys.* **16** L83–7
Marrus R and Mohr P J 1978 *Adv. At. Mol. Phys.* **14** 181–224
McWhirter R W P and Hearn A G 1963 *Proc. Phys. Soc.* **82** 641–54
Nicolosi P, Tondello G and Jannitti E 1979 *Phys. Rev.* A **20** 2574–81
Sampson D H 1977 *J. Phys. B: At. Mol. Phys.* **10** 749–60
Seely J F and Lunney J G 1982 *Opt. Commun.* **41** 43–6
Shevelko V P, Urnov A M and Vinogradov A V 1976 *J. Phys. B: At. Mol. Phys.* **9** 2859–67
Shevelko V P, Skobelev I Y and Vinogradov A V 1977 *Phys. Scr.* **16** 123–8
Skobelev I Y, Vinogradov A V and Yukov E A 1978 *Phys. Scr.* **18** 78–86
Tallents G J 1976 *Comput. Phys. Commun.* **12** 205–12
—— 1982 *Comput. Phys. Commun.* **25** 141–8
—— 1984 *Phys. Rev.* A **29** 3461–3
Tully J A 1973 *Can. J. Phys.* **51** 2047–53
Vainshtein L A 1975 *Sov. Phys.–JETP* **40** 32–5
Vinogradov A V, Sobel'man I I and Yukov E A 1974 *Sov. J. Quantum Elect.* **4** 149–54
Vinogradov A V, Skobelev I Y and Yukov E A 1977 *Sov. J. Plasma Phys.* **3** 389–94
Wiess W L, Smith M W and Glennon B M 1966 *Atomic Transition Probabilities* vol 1 (Washington: National Bureau of Standards)